PET Imaging Drug Distribution After Intratumoral Injection: The Case for ^{124}I-Iododeoxyuridine in Malignant Gliomas

Ulrich Roelcke, MD[1]; Oliver Hausmann, MD[2]; Adrian Merlo, MD[2]; John Missimer, PhD[1]; Ralph P. Maguire, PhD[1]; Peter Freitag, MD[3]; Ernst W. Radü, MD[3]; Regin Weinreich, PhD[4]; Otmar Gratzl, MD[2]; and Klaus L. Leenders, MD[1]

[1]PET Program, Paul Scherrer Institute, Villigen, Switzerland; [2]Department of Neurosurgery, University Hospital, Basel, Switzerland; [3]Department of Neuroradiology, University Hospital, Basel, Switzerland; and [4]Institute of Medical Radiobiology, Paul Scherrer Institute, Villigen, Switzerland

Locoregional administration may yield higher tumor drug concentrations compared with intravenous injection and may reduce the risk of systemic adverse effect. Furthermore, in the case of brain tumors, it may circumvent limited drug delivery imposed by the blood–brain barrier. We used PET to study the retention and spatial distribution of iododeoxyuridine (IUdR), which has been used as a DNA-targeting radiosensitizing drug and which can be charged with therapeutic nuclides. **Methods:** Locoregional (resection cavity, tumor) instillation of 5–19 MBq ^{124}I-IUdR was achieved in 7 postoperative patients with malignant gliomas through a reservoir implanted in the skull. Patients were scanned with PET during the first hour and at 2, 24, and 48 h after ^{124}I-IUdR instillation. ^{124}I-IUdR metabolism was measured in the reservoir fluid in the presence or absence of a degradation inhibitor (5′-butyryl-IUdR [butyryl-IUdR]). Region-of-interest analysis was applied to calculate intratumoral retention (K_{local}) of ^{124}I-IUdR from the PET images after a 24-h washout phase using an autoradiographic method. **Results:** At 24 h, radioactivity concentration in the reservoir was approximately 1% of the concentration 5 min after tracer instillation. The major metabolite of ^{124}I-IUdR in the reservoir was ^{124}I-iodouracil. ^{124}I-IUdR degradation could be partially inhibited by butyryl-IUdR. In the plasma, radioactivity peaked between 2 and 6 h. The area of tissue radioactivity increased with time up to 3-fold compared with the initial distribution. Tumor ^{124}I-IUdR retention (K_{local}) ranged from 0.006 to 0.017 μL/g/min, which is substantially lower compared with the IUdR-DNA incorporation reported recently after intravenous injection of ^{124}I-IUdR (K_i, 3.9 ± 2.3 μL/g/min, where K_i is the DNA incorporation rate of ^{124}I-IUdR after intravenous tracer injection). **Conclusion:** Although a single injection of ^{124}I-IUdR resulted in radioactivity distribution over the tumor, retention at 24 h was substantially lower compared with intravenous injection of ^{124}I-IUdR. Slow diffusion after locoregional administration, in contrast to fast delivery via tumor capillaries after intravenous injection, may account for our findings, resulting in a low amount of drug incorporation into DNA before degradation and washout from tissue.

Key Words: malignant brain tumor; locoregional treatment; iododeoxyuridine; PET

J Nucl Med 2002; 43:1444–1451

Malignant glioma is the most common primary brain tumor and is associated with a poor prognosis. Metastasis is very uncommon, but infiltration of peritumoral brain and rapid formation of recurrent tumor is a major hallmark of the biologic behavior and leads to a median survival of 9–12 mo for patients with glioblastoma and up to 3 y for patients with anaplastic astrocytoma (*1*).

Standard glioma treatment includes surgical decompression, postoperative radiotherapy, and systemic chemotherapy in selected patients. Efforts to improve survival have aimed at increasing tumor concentrations of various agents by locoregional (intratumoral) injection. This is of particular importance because the blood–brain barrier limits the delivery of systemically administered drugs (*2*). Locoregional treatment regimens that have been evaluated in human brain tumor patients include chemotherapeutic agents coated on biodegradable polymers (*3*), radionuclide charged monoclonal antitenascin antibodies (*4–6*) and somatostatin receptor analogs (*7*), transferrin conjugated to diphtheria toxin (*8*), and gene therapy (*9*). In the case of locoregional treatment, the molecular weight (in units of kDa) of drug is of major importance, because distribution over the tumor and peritumoral brain has to be accomplished by either diffusion for smaller (<2 kDa) molecules or convection for larger molecules (*10*). Low-molecular-weight drugs may therefore show widespread tissue distribution because convection is substantially slower compared with diffusion (*10*).

Most compounds cited above represent peptides or even proteins with high molecular weight, which in part may account for their minor effectiveness in patients with ma-

Received Mar. 11, 2002; revision accepted Jul. 9, 2002.
For correspondence or reprints contact: Ulrich Roelcke, MD, Department of Neurology, Cantonal Hospital Aarau, CH 5001 Aarau, Switzerland.
E-mail: roelcke@ksa.ch

lignant gliomas. Among compounds with low molecular weight, the pyrimidine analog iododeoxyuridine (IUdR) (0.354 kDa) has been evaluated in human brain tumor patients after continuous intravenous or intraarterial infusion. IUdR can serve as a radiosensitizer and can be charged with therapeutic nuclides—for example, the Auger electron emitter ^{123}I-iodine or ^{125}I-iodine (*11*,*12*). Evidence is emerging from animal models that intratumoral administration of IUdR charged with either ^{123}I-iodine or ^{125}I-iodine has a high antitumoral potential (*13–15*). A recent PET study measured specific retention of ^{124}I-IUdR in human brain tumor patients after intravenous injection (*16*). This retention correlated with the bromodeoxyuridine labeling index obtained from the patients, which suggests that DNA incorporation of this drug (i.e., targeting dividing tumor cells) can be measured in vivo. In the context of locoregional brain tumor therapy, the aim of our study was to compare these results with the intratumoral distribution and retention of ^{124}I-IUdR measured with PET after intratumoral instillation through a reservoir. Because drug degradation during delivery leads to decreased specific incorporation at the target site (i.e., IUdR-DNA incorporation), we also assessed the degradation of ^{124}I-IUdR in the reservoir fluid as well as degradation inhibition with the ester-prodrug 5′-butyryl-IUdR (butyryl-IUdR) (*17*).

MATERIALS AND METHODS

Patients

Seven patients with malignant gliomas were selected. For the purpose of postoperative locoregional radioimmunotherapy (*7*), a reservoir consisting of a plastic capsule (diameter, 16 mm) was implanted in the skull during surgery. This reservoir was connected to a catheter. The bore-bearing catheter tip (diameter, 1.2 mm) was placed either in the residual tumor or in the resection cavity and allowed tracer or drug penetration into the surrounding tissue. The study protocol was approved by the local Ethical Committee. Written consent was obtained from all patients.

PET Data Acquisition

^{124}I-IUdR was prepared as described (*18*). The specific activity of ^{124}I-IUdR was 92.5 GBq/μmol. A purity grade of >95% of the tracer was routinely achieved before its application (*19*). PET measurements were performed using a rotating RPT-2 PET tomograph (Siemens/CTI, Knoxville, TN). Images of raw counts were reconstructed into 47 image planes (interplane distance, 3 mm) of dimension 128 × 128 using filtered backprojection. The pixel sizes were 2.096 mm in the transaxial plane and 3.375 mm in the axial direction. The resolution of the reconstructed images was 6-mm full width at half maximum (*20*). The PET tomograph was calibrated from separate measurements with a source of known ^{124}I-iodide radioactivity concentration; the calibration constant was in agreement with that for ^{11}C and ^{18}F, taking the positron abundance of ^{124}I-iodide (25%) (*21*) into account.

Patients were pretreated with oral potassium iodide solution before the PET study to block thyroid uptake of radiolabeled iodide, the major radiolabeled plasma metabolite of ^{124}I-IUdR. Before the PET study, the head of the patient was positioned in a plastic head support to minimize movement during PET scanning. Immediately before tracer instillation, a ^{68}Ge/^{68}Ga transmission scan of 10-min duration was obtained for attenuation correction. Before the transmission scan, patients were treated with intravenous mannitol (100 mL, 20%) and dexamethasone (16 mg) to reduce the risk of intracranial pressure increase caused by subsequent tracer instillation. After obtaining the transmission scan, the patient remained on the table, which was moved outside the tomograph. As much reservoir fluid as possible was then withdrawn (aspirated) using a small needle. Thereafter, the tracer was carefully instilled by hand over 2–3 min using the same needle into the reservoir. Immediately after instillation, the table was moved back in the tomograph at the same position as for the transmission scan.

Five minutes after completion of tracer instillation, a dynamic PET study was initiated using 14 time frames (2 × 2, 12 × 4 min; total duration, 52 min). Static PET studies of 20 min each were acquired 2, 24 (all patients), and 48 h (patients 3–7) after instillation. To localize tissue radioactivity distribution, PET emission images were registered to the corresponding PET transmission images using the AIR (Automated Image Registration, head and hat) algorithm (*22*). The registered PET images were resliced using trilinear interpolation along the planes of the MR images.

Data Analysis

The following regions of interest (ROIs) were drawn from the PET images: (a) The plastic capsule implanted into the skull was termed the reservoir. (b) The area of initial tracer distribution (5 min after instillation, first time frame of the PET study) from the catheter tip into surrounding tissue was termed the source. This source was considered to represent the input function (tracer delivery to tumor). The size of this ROI was kept fixed. (c) A trace ROI was used to outline the area of maximal radioactivity distribution in tissue (including the source). This ROI varied in size depending on the time after tracer instillation. (d) An elliptic ROI was placed over the hemisphere contralateral to the tumor side for measurement of background radioactivity at 24 h. This was used for calculation of intratumoral retention (K_{local}) at 24 h (see below).

As for the previous study on proliferation measurement with PET after intravenous injection of ^{124}I-IUdR (*16*), a 24-h interval after tracer instillation was allowed for washout of nonincorporated radioactivity (non-^{124}I-IUdR–derived activity) from tissue. In analogy to the term K_i (DNA incorporation rate of ^{124}I-IUdR after intravenous tracer injection (*16*)), tracer retention 24 h after locoregional (intralesional) tracer instillation was termed K_{local}. Tumor radioactivity concentration at that time was determined using a trace ROI and did not include the source area.

Decay-corrected time–activity curves were generated for the reservoir and source ROIs. To obtain the concentration of nonmetabolized ^{124}I-IUdR concentration in the source, total source radioactivity was multiplied by the amount of the ^{124}I-IUdR fraction measured from reservoir fluid (see below). Decay-corrected radioactivity was also calculated for the tumor ROI at 24 h. For the calculation of K_{local} (μL/g/min), an autoradiographic approach was used as:

$$K_{local} = \frac{A_m^{24h}}{\int sou \cdot dt},$$

where A_m^{24h} (Bq/mL) is the background-corrected radioactivity measured in tumor obtained from the PET images 24 h after tracer instillation, and $\int sou \cdot dt$ is the IUdR concentration time integral of the source (input function [Bq/mL/min]). The calculation of K_{local}

TABLE 1
Clinical Data

Patient no.	Age (y)	Sex	Histology	Localization (side)	Resection type	Catheter length (mm)	Catheter tip position (MRI)	Radiotherapy	DEX (mg/d)
1	38	M	anAC III	Frontal (L)	B	55	Cav	*	16
2	53	M	GBM IV	Frontal (L)	P	46	Bz	†	16
3	69	F	GBM IV	Frontotemporal (L)	Gt	22	Cav	None	12
4	50	M	GBM IV	Frontotemporal (R)	P	52	Cav	None	8
5	64	F	anAC III	Frontal (R)	Gt	36	Cav	*	12
6	42	F	anAC III	Frontal (R, L)	B	33	Tumor	‡	None
7	53	M	GBM IV	Frontal (R)	P	25	Cav	§	12

*Conventional external-beam radiotherapy with 56 Gy after first tumor operation.
†Conventional external-beam radiotherapy with 56 Gy 4 wk before PET study.
‡Interstitial brachytherapy with octreotide within 2 mo before PET study.
§Interstitial brachytherapy with yttrium within 2 mo before PET study.
Histology includes anaplastic astrocytoma World Health Organization (WHO) grade III (anAC III) and glioblastoma multiforme grade IV (GBM IV). Resection type includes biopsy (B), partial (P), and gross total resection (Gt). Catheter tip position includes resection cavity (Cav), tumor, and border zone between tumor and adjacent peritumoral edema (Bz). DEX indicates daily dexamethasone dose.

assumes that IUdR-DNA–incorporated radioactivity is trapped irreversibly until at least 24 h (*16*).

Metabolites

Aspiration fluid from the reservoir and venous plasma were analyzed for the content of tracer (^{124}I-IUdR) and radiolabeled metabolites (^{124}I-iodide, ^{124}I-iodouracil). Tracer (0.4 MBq) was mixed with the aspiration fluid and incubated at 37°C. Samples were taken at 5, 20, 60, 120, and 180 min and 24 and 48 h after starting the incubation. For determination of plasma radioactivity, venous blood samples were taken at 5, 10, 15, and 60 min and 24 and 48 h after tracer instillation. All aspiration fluid and plasma samples were placed on ice immediately after collection. Total radioactivity in the aspiration fluid and plasma was measured in a well counter. High-performance liquid chromatography (HPLC) analysis (*16*) was used to determine the relative amounts of ^{124}I-IUdR and its metabolites. The retention times for tracer and metabolites were verified using unlabeled standards and ultraviolet absorption at 254 nm. The integrated peaks of tracer and metabolites were expressed in percentage of total aspirate and plasma radioactivity at sampling time.

Butyryl-IUdR was synthesized according to Narurkar and Mitra (*17*). The magnitude of IUdR degradation inhibition by butyryl-IUdR was assessed in 3 patients after incubation of aspiration fluid with 50 μL ^{124}I-IUdR ± 50 μL butyryl-IUdR at 37°C. Each sample was assayed twice for metabolite composition (HPLC) at 60, 120, and 180 min and 24 and 48 h after starting the incubation.

RESULTS

PET studies were performed between 16 and 88 d after tumor surgery. The clinical details of all 7 patients are presented in Table 1. Two patients suffered from tumor recurrence 6 y (patient 1) and 2 y (patient 5) after surgery for low-grade astrocytoma. At the time of the PET study, patients 1, 2, and 5–7 had already completed conventional postoperative external-beam radiotherapy. In patients 6 and 7, subsequent interstitial brachytherapy was applied (*7*). No patient had received chemotherapy.

The instilled radioactivity concentrations are presented in Table 2. The total instilled volume ranged between 1.5 and 5.0 mL. Tracer instillation into the reservoir was well tolerated. Radioactivity distribution in tissue is illustrated in Figure 1. In general, distribution was variable. In 1 patient, radioactivity probably spread along the catheter and reached the brain surface (Fig. 1B). In 6 of 7 patients, the radioactivity distribution area in tissue increased between 30 min and 24 h after instillation. Compared with the initial source size, this increase amounted up to 3-fold at 24 h (patient 6; Fig. 2). Between 24 and 48 h, the area of tissue radioactivity distribution tended to decline. Tumor radioactivity concentrations remained in a similar range at 24 and 48 h and amounted to 28%–78% of radioactivity measured in the source (see below). In the contralateral brain (background), radioactivity declined in parallel with the time course in the reservoir and source. Relative to the values 5 min after instillation, a mean of 68.1% was measured after 1 h, 57.1% after 2 h, 4.8% after 24 h, and 1.7% after 48 h. Counting rates of the background ranged between 0.5% and 1% of the rates measured in the source.

In all patients, the reservoir and source were visualized on the PET images. An example of the time course of radioactivity in these ROIs is presented in Figure 3. Depending on the dose administered, initial radioactivity concentration in the reservoir ranged from 15 to 155 kBq/mL and in the source ranged from 62 to 535 kBq/mL. Relative to the value measured 5 min after ^{124}I-IUdR instillation, total radioactivity in both ROIs followed a uniform decline to 0.9% ± 0.9% at 24 h and 0.1% ± 0.1% at 48 h (mean ± SD; Fig. 3). This decline was independent of the administered dose. Figure 4A shows the metabolism of ^{124}I-IUdR during incu-

TABLE 2
Results

Patient no.	Instilled dose (MBq)	Instilled radioactivity concentration (MBq/mL)	PET source size (mm^2)	Tumor radioactivity distribution at 24 h (mm^2)	K_{local} ($\mu L/g/min$)
1	4	2.8	195	547	0.006
2	5	2.3	166	373	0.017
3	5	1.3	519	727	0.009
4	4	1.5	359	369*	—
5	19	4.7	483	724	0.008
6	19	4.0	434	912	0.016
7	19	3.7	660	769	0.010

*No significant spread of radioactivity over tumor; K_{local} could not be measured.
K_{local} = local (intratumoral) ^{124}I-IUdR retention at 24 h.

bation in the reservoir fluid. Compared with tracer degradation after intravenous tracer injection (mean plasma clearance half-time, 2.5 min (*16*)), degradation in the reservoir fluid was much slower, with a mean ^{124}I-IUdR fraction of 60% at 24 h and 50% at 48 h. In contrast to degradation in the plasma, the major metabolite was ^{124}I-iodouracil, whereas the proportion of ^{124}I-iodide remained $<$15% at 48 h. The influence of butyryl-IUdR on the degradation of ^{124}I-IUdR was studied in 3 patients (Fig. 4B). In 2 patients, this prodrug reduced the degradation of ^{124}I-IUdR by approximately 15% at 2, 3, and 24 h after starting the incubation. In the presence of the prodrug, ^{124}I-iodouracil formation was approximately 20% lower than that in the nontreated reservoir fluid. ^{124}I-Iodide formation was similar in both conditions. No effect was observed in the third patient.

The IUdR tissue retention rate, K_{local}, was derived from the 24-h PET images and the metabolite-corrected time–activity curve of the source (input function; Fig. 3). At 24 h, substantial tumor radioactivity washout was observed,

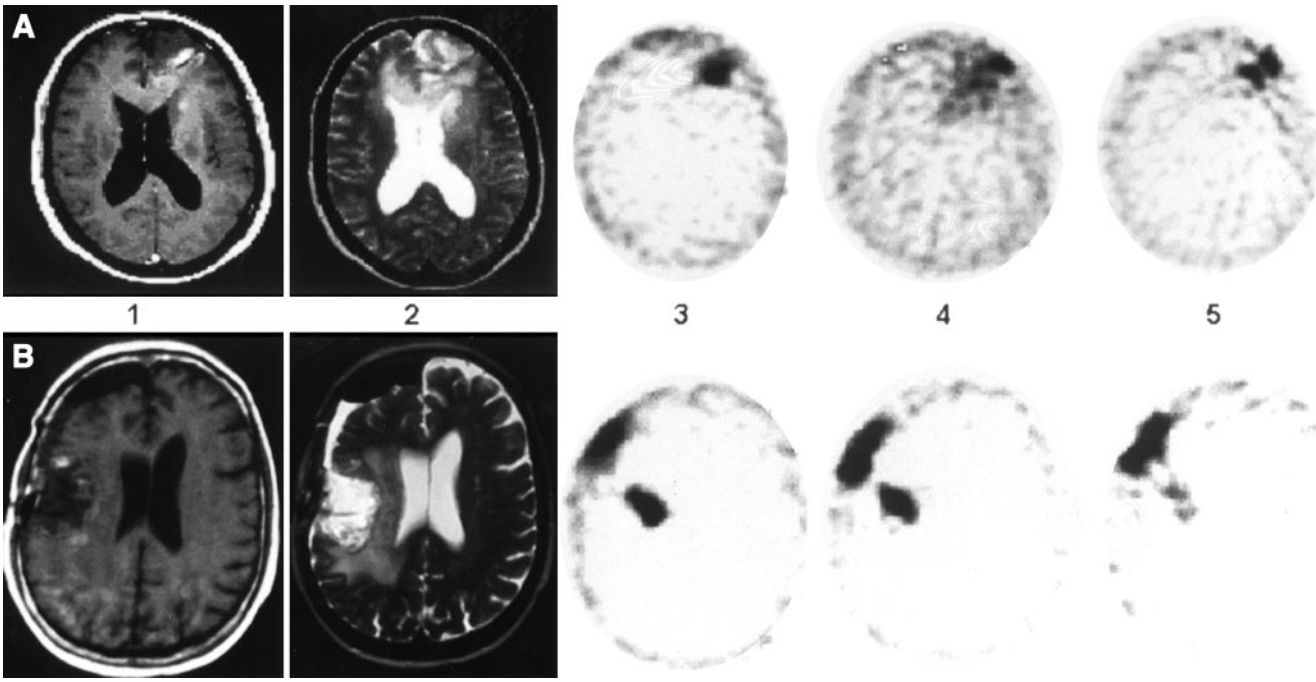

FIGURE 1. To illustrate tissue radioactivity distribution, PET emission images acquired 5 min (no. 3), 24 h (no. 4), and 48 h (no. 5) after tracer instillation are coaligned with contrast-enhanced T1-weighted (no. 1) and T2-weighted (no. 2) MR images. Because radioactivity 24 and 48 h after tracer instillation decreased to approximately 5%–10% of initial values, each PET image is calibrated to its own maximum. (A) Patient 6: Radioactivity distributes over tumor and partially covers peritumoral T2 hyperintense brain at 24 h. Reservoir (skull) and source (adjacent parenchyma) are visualized. (B) Patient 4: Reservoir and catheter are seen (nos. 1 and 2). Radioactivity does not distribute over tumor but spreads along brain surface (nos. 3–5).

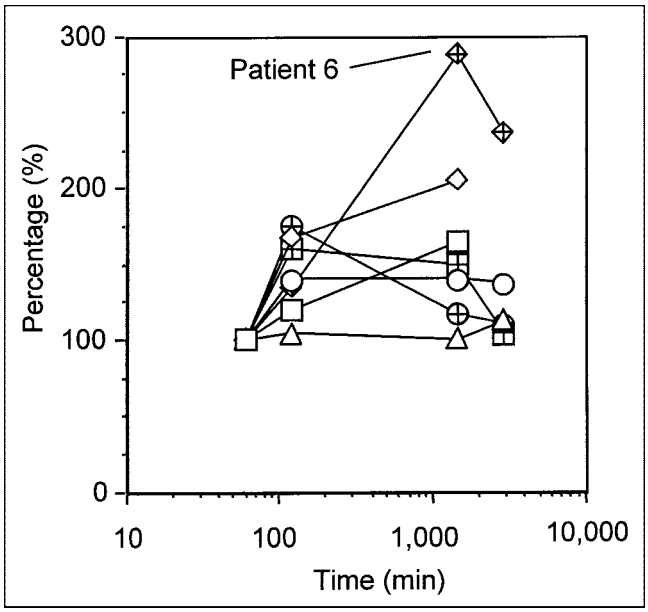

FIGURE 2. Time course of tissue radioactivity distribution (percentage of area size at 5 min). Each symbol represents 1 individual patient. Patient 6: catheter tip placed in tumor parenchyma.

which was similar to the radioactivity washout measured in the source ROI. K_{local} was comparable in anaplastic astrocytoma and glioblastoma and ranged from 0.006 to 0.017 μL/g/min (Table 2). The 2 patients with the catheter tip either in tumor parenchyma or at the border zone (patients 2 and 6, Table 1) showed the highest K_{local}. Overall, however, K_{local} was substantially lower than the mean K_i obtained after intravenous ^{124}I-IUdR injection reported earlier (3.9 μL/g/min (*16*)).

Venous plasma radioactivity peaked between 2 and 6 h after tracer instillation (data not shown). Depending of the administered dose, peak concentrations ranged from 88 ± 20 Bq/mL to 296 ± 159 Bq/mL. This radioactivity was represented by ^{124}I-iodide only (HPLC). At 24 and 48 h, plasma radioactivity was still detectable, which constituted 36% and 16% of the peak concentrations, respectively.

DISCUSSION

Our study on the spatial distribution and kinetics of the tracer and drug ^{124}I-IUdR demonstrates that a single locoregional bolus instillation of a low-molecular-weight DNA-targeting compound results in a variable tissue distribution, substantial tracer clearance from tissue, and a lower fraction of radioactivity retention in tumor compared with the tumor DNA incorporation of ^{124}I-IUdR after intravenous injection (*16*). With the background that theoretically higher drug concentrations can be achieved by locoregional instillation and that IUdR was clinically ineffective in brain tumor patients even after continuous intravenous infusion (*23*,*24*), but induced tumor regression in animal models after intratumoral administration (*14*,*25*), our results are at the moment disappointing from a clinical point of view. The heterogeneity of our patient group with regard to postoperative radiotherapy and chemotherapy, composition of residual tumor and peritumoral edema, and catheter tip position may contribute to these results because these factors influence tracer distribution and binding. In addition, with our study design it is not possible to validate K_{local} by independent tissue analysis as presented earlier (*16*). Nevertheless, several methodologic issues that are relevant to the evaluation of locoregional brain tumor treatment can be addressed.

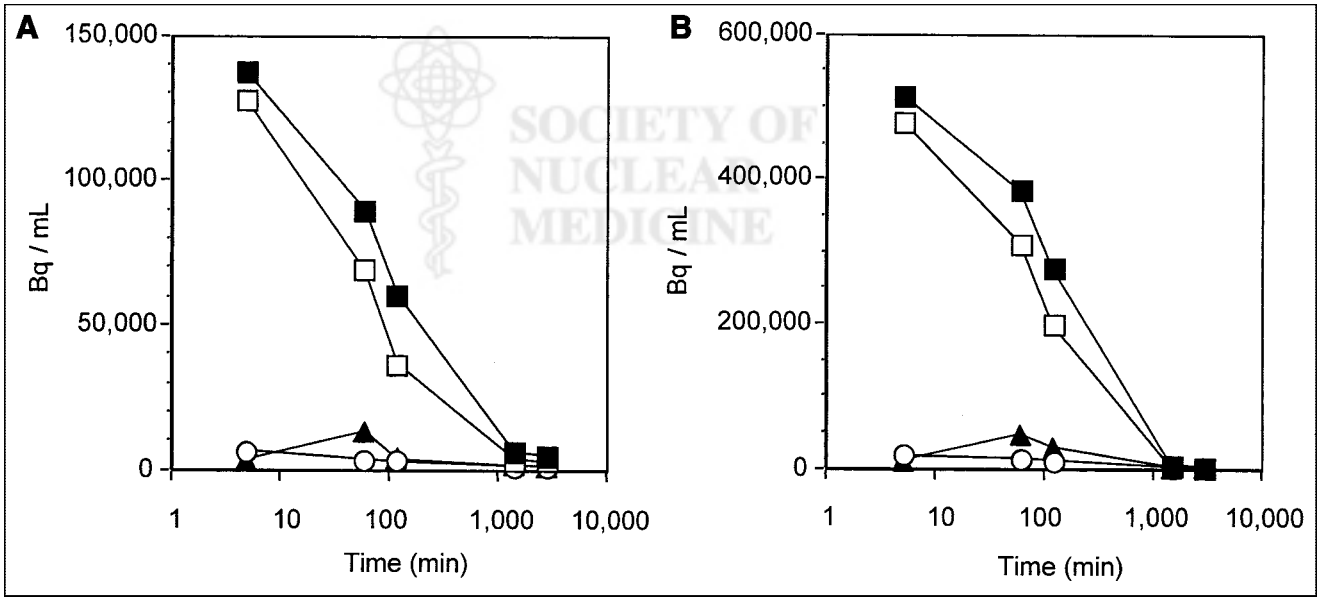

FIGURE 3. Decay-corrected time–activity curve for reservoir (A) and source (B) in patient 5. ■, Total radioactivity; metabolite time–activity curve: □, ^{124}I-IUdR; ○, ^{124}I-iodide; ▲, ^{124}I-iodouracil.

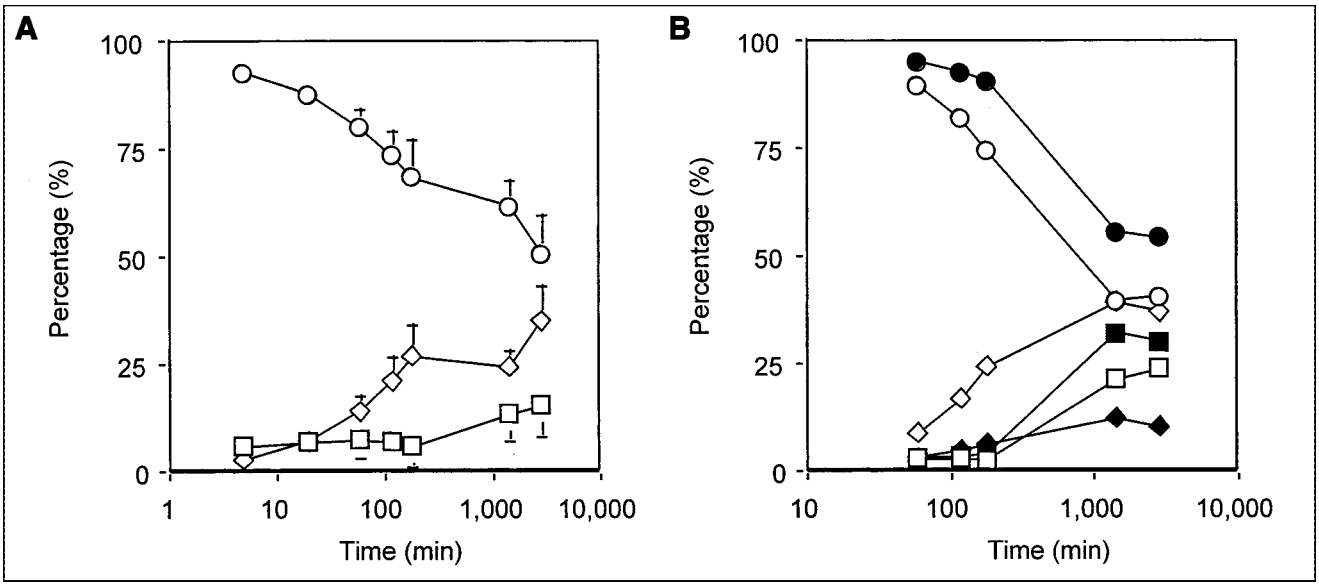

FIGURE 4. (A) Time course of ^{124}I-IUdR degradation and metabolite formation in aspiration fluid of all 7 patients (mean ± SEM). (B) Effect of butyryl-IUdR on metabolite formation (means of 3 patients, each sample assayed twice). ○ and ●, ^{124}I-IUdR; ◇ and ◆, ^{124}I-iodouracil; □ and ■, ^{124}I-iodide; ○, ◇, and □, without coincubation; ●, ◆, and ■, after coincubation of ^{124}I-IUdR and butyryl-IUdR (B).

To our knowledge, this is the first study using PET to quantify tumor tracer distribution after locoregional instillation in human brain tumor patients. We used the compartment initially occupied by ^{124}I-IUdR (the source) for calculation of the metabolite-corrected input function, which represents radioactivity released from the catheter tip into the resection cavity. Allowing tracer distribution from the source and washout of nonspecific radioactivity from the tumor tissue (*16*), local tracer retention (K_{local}) could be calculated in 6 of 7 patients. In 1 patient, the size of the source radioactivity did not change substantially over the measurement period, which makes it unlikely that measurable specific tumor uptake occurred in this patient (patient 4). Evaluating different modes of tracer application, Mairs et al. (*15*) showed in an animal brain tumor model that single intratumoral injection of 0.37 MBq ^{125}I-IUdR labeled only 6% of tumor cells, whereas similar amounts of ^{125}I-IUdR released from polymer or infused continuously via an osmotic pump labeled 22% and 34% of tumor cells, respectively. This finding illustrates that, although most tumor radioactivity in animal models is recovered from DNA (*26*), the volume of tumor targeted by IUdR depends on the mode of administration and approaches one third at the maximum (*15*). It is conceivable that in the case of human brain tumors that exhibit a low-to-moderate proliferation rate (*1*) only a small amount of ^{124}I-IUdR is in fact incorporated into tumor cell DNA. Therefore, continuous release of tracer also must be envisaged in human patients. Preliminary data show the feasibility of this approach (*8*).

The source was used as the input function for the determination of K_{local}. Radioactivity in this ROI decreased uniformly by 50% within 2 h and approached 1% of initial radioactivity at 24 and 48 h after instillation (Fig. 3). The maximum of plasma radioactivity that consisted of ^{124}I-iodide occurred within the first 4–6 h and suggests major radioactivity clearance from the source within that time. This is in line with observations from an ^{123}I-IUdR SPECT study on 1 patient with low-grade glioma, in which plasma ^{123}I-iodide concentration peaked within 8 h. Approximately 80% of locoregionally instilled radioactivity was found in the urine of this patient (*27*). Accordingly, we assume that only a minor proportion of instilled tracer was available for distribution over the tumor in our patients. To evaluate the pattern of metabolic degradation of ^{124}I-IUdR that could occur in the source region and adjacent tissue, we analyzed the fractions of ^{124}I-IUdR and its metabolites during tracer incubation in the reservoir fluid, which was taken immediately before tracer instillation. In contrast to the rapid plasma metabolism of ^{124}I-IUdR, where ^{124}I-iodide represented >80% of total plasma radioactivity 20 min after intravenous injection (*16*), much slower degradation was observed in the reservoir: Only 50% of ^{124}I-IUdR was metabolized after 48 h, and ^{124}I-iodouracil was the major metabolite (Fig. 4A). Coincubation of butyryl-IUdR and ^{124}I-IUdR in the reservoir fluid reduced ^{124}I-IUdR degradation in 2 of 3 patients by 15% at 24 h (Fig. 4B). Butyryl-IUdR, which was developed to enhance the efficacy of intraparenchymal IUdR against herpes simplex encephalitis, inhibited completely IUdR degradation in rat brain over 6 h (*28*). Our results that were obtained from the reservoir fluid suggest that butyryl-IUdR may also increase the concentration of locoregionally administered IUdR in tumor tissue of human patients.

A yet unresolved debate exists relating to the physicochemical properties of brain tumor-targeting drugs. As far as the molecular weight is concerned, compounds with low molecular weight may have the advantage of rapid and widespread tissue distribution but may also be prone to rapid washout before binding to their target. Alternatively, compounds with high molecular weight may be exposed longer to their target because of a longer residence time in tissue. At the moment, few in vivo data address drug tumor tissue distribution after locoregional administration, clinical response, or both. Merlo et al. (*7*) used doses of 100 MBq of the somatostatin analog ^{111}In-octreotide (1.3 kDa) and planar scintigraphy and noted an "extensive" distribution of the compound over the entire tumor (low-grade and malignant gliomas). With ^{123}I-IUdR (0.354 kDa), 1 patient with low-grade glioma was studied with planar scintigraphy (injected dose, 141.3 MBq [3.82 mCi]) (*27*). The authors did not comment on the extent of tracer distribution with regard to tumor size but observed a steady decline of the difference between tumor and normal brain radioactivity over 52 h, which suggests minor or no specific DNA incorporation of the tracer. In this study, radioactivity distribution over the tumor was variable. Compared with the initial size of the source radioactivity, increases of up to 3-fold were found (Fig. 2). It could be questioned whether the low-activity doses instilled in our patients (4–19 MBq) may in part account for the failure to cover the whole tumor area by ^{124}I-IUdR–derived radioactivity. In this case, more widespread tumor radioactivity would not be detected because of the sensitivity of the PET camera. On the other hand, ^{124}I-IUdR washout into the circulation may dominate over ^{124}I-IUdR diffusion from the source into the tumor, particularly in those patients with the catheter tip located in the resection cavity. This is supported by the observation that the patients with the catheter tip located in the tumor parenchyma (patients 2 and 6) showed the highest values of K_{local}.

A stable (several days) radioactivity distribution over the tumor was observed in studies using ^{131}I-iodine–labeled (*29*) or ^{111}In-indium–labeled (*4*) antitenascin antibodies and ^{131}I-iodine–labeled neural cell adhesion molecule antibody (*30*). Persisting distribution of these high-molecular-weight compounds over the tumor indicates that washout into the circulation is much slower compared with that of IUdR. Although it has not been shown that these molecules in fact reach their biochemical target, their local residence time may then at least prolong the exposure of therapeutic irradiation to the tumor. Preliminary results from studies in brain tumor patients indicated increasing survival times using this approach (*5*,*6*). Taken together, the advantage of low molecular weight, as for IUdR, may be irrelevant if rapid washout from tissue dominates over diffusion through the tumor after locoregional administration. This may yield even lower specific drug binding to the target compared with systemic administration of the same compound, where the blood–brain barrier permeability and tissue perfusion are critical to drug delivery.

CONCLUSION

The combination of tomographic and pharmacokinetic assessment of drugs administered locoregionally in tumor patients in our pilot PET study is feasible and appears worthwhile to pursue more extensively. To account for patient heterogeneity, at least subjects with the catheter tip located in the tumor parenchyma should be selected. Because tissue clearance has to be expected, particularly for low-molecular-weight compounds after locoregional administration, further studies must clarify whether osmotic substances are required immediately before tracer instillation because they may open the blood–brain barrier and enhance tracer washout from tissue ("sink" effect). With regard to the targeted tumor volume, the mode of administration (bolus vs. continuous) and the tracer concentration have to be addressed. We expect that this type of study will contribute significantly to understanding the failure and options of local brain tumor treatment.

ACKNOWLEDGMENTS

The authors gratefully acknowledge the help of Leo Wyer (Institute of Medical Radiobiology) in radiosynthesis of ^{124}I-IUdR, of Dr. Mario Argentini (Institute of Medical Radiobiology) in synthesis of butyryl-IUdR, and of Claudia Vetter (PET Program, Paul Scherrer Institute) in performing HPLC analysis. Peter Vontobel (PET Program, Paul Scherrer Institute) participated in the discussion of kinetic PET data.

REFERENCES

1. De Angelis LM. Brain tumors. *N Engl J Med.* 2001;344:114–123.
2. Pardridge W. Drug delivery to the brain. *J Cereb Blood Flow Metab.* 1997;17:713–731.
3. Brem H, Piantadosi S, Burger PC, et al. Placebo-controlled trial of safety and efficacy of intraoperative controlled delivery by biodegradable polymers of chemotherapy for recurrent gliomas. *Lancet.* 1995;345:1008–1012.
4. Merlo A, Jermann E, Hausmann O, et al. Biodistribution of ^{111}In-labelled SCN-bz-DTPA-BC-2 MAb following loco-regional injection into glioblastomas. *Int J Cancer.* 1997;71:810–816.
5. Riva P, Franceschi G, Riva N, Casi M, Santimaria M, Adamo M. Role of nuclear medicine in the treatment of malignant gliomas: the locoregional radioimmunotherapy approach. *Eur J Nucl Med.* 2000;27:601–609.
6. Cokgor I, Akabani G, Kuan CT, et al. Phase I trial results of iodine-131-labeled antitenascin monoclonal antibody 81C6 treatment of patients with newly diagnosed malignant gliomas. *J Clin Oncol.* 2000;18:3862–3872.
7. Merlo A, Hausmann O, Wasner M, et al. Locoregional regulatory peptide receptor targeting with the diffusible somatostatin analogue ^{90}Y-labeled DOTA0-D-Phe1-Tyr3-octreotide (DOTATOC): a pilot study in human gliomas. *Clin Cancer Res.* 1999;5:1025–1033.
8. Laske DW, Youle RJ, Oldfield EH. Tumor regression with regional distribution of the targeted toxin TF-CRM107 in patients with malignant brain tumors. *Nat Med.* 1997;3:1362–1368.
9. Gupta N. Current status of viral gene therapy for brain tumours. *Expert Opin Investig Drugs.* 2000;9:713–726.
10. Jain RK. Transport of molecules in the tumor interstitium. *Cancer Res.* 1987;47:3039–3051.
11. Bloomer WD, Adelstein SJ. 5-^{125}I-Iododeoxyuridine as prototype for radionuclide therapy with Auger emitters. *Nature.* 1977;265:620–621.
12. Sastry KS. Biological effects of the Auger emitter iodine-125: a review. Report

No. 1 of AAPM Nuclear Medicine Task Group No. 6. *Med Phys.* 1992;19:1361–1370.
13. Kassis AI, Van den Abbeele AD, Wen PY, et al. Specific uptake of the Auger electron-emitting thymidine analogue 5-[^{123}I/^{125}I]iodo-2′-deoxyuridine in rat brain tumors: diagnostic and therapeutic implications in humans. *Cancer Res.* 1990;50:5199–5203.
14. Kassis AI, Wen PY, Van den Abbeele AD, et al. 5-[^{125}I]Iodo-2′-deoxyuridine in the radiotherapy of brain tumors in rats. *J Nucl Med.* 1998;39:1148–1154.
15. Mairs RJ, Wideman CL, Angerson WJ, et al. Comparison of different methods of intracerebral administration of radioiododeoxyuridine for glioma therapy using a rat model. *Br J Cancer.* 2000;82:74–80.
16. Blasberg RG, Roelcke U, Weinreich R, et al. Imaging brain tumor proliferative activity with [^{124}I]iododeoxyuridine. *Cancer Res.* 2000;60:624–635.
17. Narurkar MM, Mitra AK. Synthesis, physicochemical properties, and cytotoxicity of a series of 5′-ester prodrugs of 5-iodo-2′-deoxyuridine. *Pharm Res.* 1988;5:734–736.
18. Knust EJ, Dutschka K, Weinreich R. Preparation of ^{124}I solutions after thermodistillation of irradiated $^{124}TeO_2$ targets. *Appl Radiat Isot.* 2000;52:181–184.
19. Guenther I, Wyer L, Knust EJ, Finn RD, Koziorowski J, Weinreich R. Radiosynthesis and quality assurance of 5-[^{124}I]iodo-2′-deoxyuridine for functional PET imaging of cell proliferation. *Nucl Med Biol.* 1998;25:359–365.
20. Townsend DW, Byars LG, Defrise M, et al. Design and performance of a rotating positron tomograph, RPT-2. In: Klaisner LA, ed. *IEEE Nuclear Science Symposium and Medical Imaging Conference Record.* San Francisco, CA: The Institute of Electrical and Electronics Engineers; 1993:1058–1062.
21. Lederer CM, Shirley VS, Browne E. *Table of Isotopes.* 7th ed. New York, NY: Wiley; 1978:69.
22. Woods JC, Mazziotta SR. MRI-PET registration with automated algorithm. *J Comp Assist Tomogr.* 1993;17:536–546.
23. Goffman TE, Dachowski LJ, Bobo H, et al. Long-term follow-up on National Cancer Institute Phase I/II study of glioblastoma multiforme treated with iododeoxyuridine and hyperfractionated irradiation. *J Clin Oncol.* 1992;10:264–268.
24. Kinsella TJ, Collins J, Rowland J, et al. Pharmacology and phase I/II study of continuous intravenous infusions of iododeoxyuridine and hyperfractionated radiotherapy in patients with glioblastoma multiforme. *J Clin Oncol.* 1988;6:871–879.
25. Yuan X, Dillehay LE, Williams JR, Williams JA. IUdR polymers for combined continuous low-dose rate and high-dose rate sensitization of experimental human malignant gliomas. *Int J Cancer.* 2001;96:118–125.
26. Tjuvajev J, Muraki A, Ginos J, et al. Iododeoxyuridine uptake and retention as a measure of tumor growth. *J Nucl Med.* 1993;34:1152–1162.
27. Kassis AI, Tumeh SS, Wen PY, et al. Intratumoral administration of 5-[^{123}I]iodo-2′-deoxyuridine in a patient with a brain tumor. *J Nucl Med.* 1996;37(suppl 4):19S–22S.
28. Ghosh MK, Mitra AK. Brain parenchymal metabolism of 5-iodo-2′-deoxyuridine and 5′-ester prodrugs. *Pharm Res.* 1992;9:1048–1052.
29. Riva P, Franceschi G, Frattarelli M, et al. ^{131}I radioconjugated antibodies for the locoregional radioimmunotherapy of high-grade malignant glioma: phase I and II study. *Acta Oncol.* 1999;38:351–359.
30. Papanastassiou V, Pizer BL, Coakham HB, et al. Treatment of recurrent and cystic malignant gliomas by a single intracavity injection of ^{131}I monoclonal antibody: feasibility, pharmacokinetics and dosimetry. *Br J Cancer.* 1993;67:144–151.